

Frequency decomposition of astrometric signature of planetary systems

Maciej Konacki ¹,

*Department of Geological and Planetary Sciences, California Institute of Technology, 1201 E.
California Blvd., Pasadena, CA 91125, USA*

Andrzej J. Maciejewski ²

*Toruń Centre for Astronomy, Nicolaus Copernicus University,
87-100 Toruń, Gagarina 11, Poland*

Alex Wolszczan ³

*Department of Astronomy and Astrophysics, Penn State University
University Park, PA 16802, USA*

*Toruń Centre for Astronomy, Nicolaus Copernicus University
ul. Gagarina 11, 87-100 Toruń, Poland*

ABSTRACT

We present theoretical analysis of the astrometric searches for extrasolar planets with the Space Interferometry Mission (SIM). Particularly, we derive a model for the future measurements with SIM and discuss the problem of reliable estimation of orbital elements of planets. For this purpose we propose a new method of data analysis and present a numerical test of its application on simulated SIM astrometric measurements of ν Andromedae planetary system. We demonstrate that our approach allows successful determination of its orbital elements.

Subject headings: astrometry — methods: data analysis — planetary systems

1. Introduction

One of the most important and challenging goals of the Space Interferometry Mission (SIM, see <http://sim.jpl.nasa.gov/>) is astrometric detection of extrasolar planetary systems including Earth-like planets around stars from the solar neighborhood. High precision astrometry requires not only advanced technology but also adequately elaborated methods of data analysis. Among

¹e-mail: maciej@gps.caltech.edu

²e-mail: maciejka@astri.uni.torun.pl

³e-mail: alex@astro.psu.edu

others it is important to develop techniques allowing reliable detection of planetary signatures and extraction of the orbital elements. The aim of this paper is to discuss some of the problems related to this subject. Specifically, we propose a method called the Frequency Decomposition (FD) to detect planets and help to obtain their orbital elements. This method has been successfully used for PSR 1257+12 timing observations (Konacki, Maciejewski & Wolszczan 1999) and 16 Cygni B radial velocity measurements (Konacki and Maciejewski 1999). Particular nature of the astrometric observations requires however some modifications of our original approach. In the paper we present a theoretical background of the method and an example of its application.

The astrometric signal is a superposition of several effects of different magnitude and a proper analysis of the observations requires at least rough a priori knowledge of how different effects contribute to the signal. However, these effects depend on the parameters (such as number of planets, their eccentricities) which are unknown in advance. So what we propose is a two-step analysis (1) FD to understand the basic properties of the signal (i.e determine the number of planets and approximate values of their orbital elements) and (2) least-squares fit based on a proper model and the starting values of parameters derived from the previous step to refine the parameters and obtain their uncertainties.

The basic idea of FD is the following. With few exception (proper motion, long period planets) the processes contributing to the signal are periodic. Therefore our astrometric signal can be successfully modeled as a multiple Fourier series plus a polynomial of certain degree (to account for the proper motion and long period planets). FD is a numerical algorithm to obtain the estimates of frequencies, amplitudes and phases of such model (Konacki, Maciejewski & Wolszczan 1999). Let us note that such approach, contrary to the usual least-squares method, allows us to analyze the data without assuming any physical model. Subsequently we interpret derived parameters. We decide how many planets are present in the system and calculate their orbital parameters (as one can derive analytical formula expressing amplitudes and phases as functions of the orbital elements). This is especially useful for multiple planetary systems where deciphering the number of planets may be tricky (e.g. two planets in circular 2:1 resonant orbits may mimic one planet in an eccentric orbit, see Konacki and Maciejewski 1999). Our approach can be also helpful while trying to determine whether we observe an astrometric displacement from a planet in 1-yr orbit or annual parallax since the parallactic motion has its own specific Fourier expansion constrained by SIM orbit. Finally, we can use these findings to perform the 'traditional' least-squares fit. We believe that such approach allows us to make more justified hypothesis about the data and in consequence lead to reliable results.

The plan of our paper is the following. In section 2 we derive a detailed model of the SIM measurements. In section 3 we investigate Fourier properties of the orbital motion. In section 4 we discuss our approach to the analysis of SIM data and finally in section 5 we perform some numerical tests to show how our method works in practice.

2. Modeling delays

SIM measures relative positions of stars using Michelson interferometers. A single measurement with SIM gives the projection of direction to the star \mathbf{s} onto the interferometer baseline vector \mathbf{B} . The measured quantity is the optical pathlength delay between the two arms of the interferometer (Shao & Baron 1999)

$$d = \mathbf{B} \cdot \mathbf{s} + c + \epsilon, \quad (1)$$

where c is the zero point of the metrology gauge and ϵ represents measurement uncertainty. The search for extrasolar planet is performed in so-called narrow angle mode where delays toward two stars (called target and reference) within 1° are measured and compared. For this kind of observation the measured quantity becomes the relative delay

$$D = \mathbf{B} \cdot (\mathbf{s}_1 - \mathbf{s}_2) + \epsilon, \quad (2)$$

where \mathbf{s}_1 and \mathbf{s}_2 are directions to the target and reference stars, respectively. Such narrow-angle measurement gives the angular separation between the stars and offers higher accuracy as many errors scale with the angular distance.

The direction to a star $\mathbf{S} = \mathbf{S}(t)$ from the Solar System Barycenter (SSB) is changing with time due to the proper motion and presence of companions. These two effects, we model in the following way

$$\mathbf{S}(t) = \mathbf{S}_0 + \delta\mathbf{S}_\mu(t) + \delta\mathbf{S}_c(t), \quad (3)$$

where \mathbf{S}_0 is the direction toward the star at epoch t_0 ; $\delta\mathbf{S}_\mu(t)$ and $\delta\mathbf{S}_c(t)$ describe changes due to the proper and orbital motion, respectively. In order to properly calculate these changes let us assume that the SSB radius vector of each star is given by

$$\mathbf{R} = \mathbf{R}_0 + \delta\mathbf{R}, \quad \text{where } \|\delta\mathbf{R}\| \ll \|\mathbf{R}_0\|, \quad (4)$$

then up to the first order in $\|\delta\mathbf{R}\|/\|\mathbf{R}_0\|$

$$\mathbf{S} = \frac{\mathbf{R}}{\|\mathbf{R}\|} = \mathbf{S}_0 + \delta\mathbf{S}^{(1)}, \quad (5)$$

where

$$\mathbf{S}_0 = \frac{\mathbf{R}_0}{\|\mathbf{R}_0\|}, \quad \delta\mathbf{S}^{(1)} = -\frac{1}{\|\mathbf{R}_0\|} \mathbf{S}_0 \times (\mathbf{S}_0 \times \delta\mathbf{R}), \quad (6)$$

The correction $\delta\mathbf{S}^{(1)}$ can be written in the form

$$\delta\mathbf{S}^{(1)} = \frac{1}{\|\mathbf{R}_0\|} [\delta\mathbf{R} - \mathbf{S}_0(\mathbf{S}_0 \cdot \delta\mathbf{R})] = \frac{1}{\|\mathbf{R}_0\|} \delta\mathbf{R}_\perp, \quad (7)$$

which means that it only depends on the component of $\delta\mathbf{R}$ perpendicular to \mathbf{S}_0 . It turns out that sometimes the first order correction is not sufficient. Therefore we need to derive and analyze also the second order term $\delta\mathbf{S}^{(2)}$ given by

$$\delta\mathbf{S}^{(2)} = \mathbf{S}_0 \left[\frac{3}{2} \left(\mathbf{S}_0 \cdot \frac{\delta\mathbf{R}}{\|\mathbf{R}_0\|} \right)^2 - \frac{1}{2} \left(\frac{\|\delta\mathbf{R}\|}{\|\mathbf{R}_0\|} \right)^2 \right] - \frac{\delta\mathbf{R}}{\|\mathbf{R}_0\|} \left(\mathbf{S}_0 \cdot \frac{\delta\mathbf{R}}{\|\mathbf{R}_0\|} \right) \quad (8)$$

If we represent $\delta\mathbf{R}$ as a sum of two components, perpendicular and parallel to \mathbf{S}_0 ,

$$\delta\mathbf{R} = \delta\mathbf{R}_\perp + \delta\mathbf{R}_\parallel \quad (9)$$

$\delta\mathbf{S}^{(2)}$ can be written as

$$\delta\mathbf{S}^{(2)} = -\frac{1}{2} \left(\frac{\|\delta\mathbf{R}_\perp\|}{\|\mathbf{R}_0\|} \right)^2 \mathbf{S}_0 - \frac{\|\delta\mathbf{R}_\parallel\|}{\|\mathbf{R}_0\|^2} \delta\mathbf{R}_\perp \quad (10)$$

As we show in section 2.3, $\delta\mathbf{S}^{(2)}$ is especially significant for nearby stars with large proper motions. For such stars we have

$$\delta\mathbf{R}_\perp = \mathbf{V}_T t \quad \delta\mathbf{R}_\parallel = \mathbf{V}_R t \quad (11)$$

where \mathbf{V}_T and \mathbf{V}_R are respectively transverse and radial velocity of the star. Thus if the star has a significant proper motion, through astrometric observations we can detect angular displacement $\delta\theta$ (second term in equation (10))

$$\delta\theta = \frac{\|\delta\mathbf{R}_\parallel\|}{\|\mathbf{R}_0\|} \frac{\|\delta\mathbf{R}_\perp\|}{\|\mathbf{R}_0\|} = \frac{\|\mathbf{V}_T\|}{\|\mathbf{R}_0\|} \frac{\|\mathbf{V}_R\|}{\|\mathbf{R}_0\|} t^2 \quad (12)$$

due to the radial velocity. This effect is called *perspective acceleration*. The other term from the equation (10) has an interesting property. Namely, it can be shown that it does not change the angle between $\mathbf{S}(t) = \mathbf{S}_0 + \delta\mathbf{S}^{(1)}(t) + \delta\mathbf{S}^{(2)}(t)$ and \mathbf{S}_0 (i.e. current and initial position of the star). In other words, if we had a direct way to measure this angle, we would not observe any effect from that term. However, since we measure all angles through the equation (1) and model the unit vector toward the star with $\mathbf{S}(t) = \mathbf{S}_0 + \delta\mathbf{S}^{(1)}(t) + \delta\mathbf{S}^{(2)}(t)$, the term $-\frac{1}{2} (\|\delta\mathbf{R}_\perp\|/\|\mathbf{R}_0\|)^2 \mathbf{S}_0$ is necessary. Specifically it affects the length of the vector \mathbf{S} and helps to keep it normalized within the accuracy of the second order approximation. Further details concerning second order corrections we discuss in section 2.3.

2.1. Local frame and baseline vector orientations

In order to obtain explicit form of the delay d we need to calculate a scalar product $\mathbf{B} \cdot \mathbf{S}$. The value of this product does not depend on a chosen reference frame. Thus, depending on our needs we can express vectors on the right hand side of (3) in different ways. It is convenient to introduce a local right hand orthonormal frame at the point \mathbf{S}_0 on the celestial sphere (see Fig. 1).

This frame is connected with the classical equatorial spherical coordinates and is defined by the unit vectors $\{\mathbf{e}_\alpha, \mathbf{e}_\delta, \mathbf{e}_r\}$. In SSB equatorial frame coordinates of these vectors are the following

$$\mathbf{e}_\alpha = (-\sin \alpha, \cos \alpha, 0), \quad \mathbf{e}_\delta = (-\sin \delta \cos \alpha, -\sin \delta \sin \alpha, \cos \delta), \quad (13)$$

$$\mathbf{e}_r = \mathbf{S}_0 = (\cos \delta \cos \alpha, \cos \delta \sin \alpha, \sin \delta), \quad (14)$$

where $(\alpha, \delta) = (\alpha_0, \delta_0)$ is the right ascension and declination of a star at t_0 .

One can determine the relative position of the target and reference star using two interferometers or, as it is planned for SIM, by performing two measurements with one interferometer for two non parallel orientations of its baseline, \mathbf{B}_i , $i = 1, 2$. For each orientation, the baseline can be represented as a sum of two vectors, $\mathbf{B}_i^{\parallel}, \mathbf{B}_i^{\perp}$, parallel and perpendicular to the initial direction toward the target star, \mathbf{S}_0 . Since we have $\mathbf{S}(t) = \mathbf{S}_0 + \delta\mathbf{S}(t)$ where $\delta\mathbf{S}(t)$ is a displacement tangent to \mathbf{S}_0 , the delay can be written as

$$d = \mathbf{B}_i \cdot \mathbf{S}(t) + c + \epsilon = \mathbf{B}_i^{\parallel} \cdot \mathbf{S}_0 + \mathbf{B}_i^{\perp} \cdot \delta\mathbf{S}(t) + c + \epsilon = d_0 + \Delta d(t) + c + \epsilon \quad (15)$$

where $d_0 = \mathbf{B}_i^{\parallel} \cdot \mathbf{S}_0$ and $\Delta d(t) = \mathbf{B}_i^{\perp} \cdot \delta\mathbf{S}(t)$. Clearly, from the planet detection point of view the important term is $\Delta d(t)$. Assuming that the measurement uncertainty, ϵ , is independent on the baseline orientation the most favorable orientation of \mathbf{B}_i is $\mathbf{B}_i = \mathbf{B}_i^{\perp}$. For such orientation $\Delta d(t)$ is the largest possible for a given length of the baseline. Moreover, the baseline orientations should be perpendicular. This way the the covariance ellipse on the sky will be circular and there will not be any direction on the plane tangent at \mathbf{S}_0 in which the measurements are more accurate than in others. Therefore, for all further considerations we assume that all observations are made with two orthogonal and fixed baseline orientations \mathbf{B}_1 and \mathbf{B}_2 which are perpendicular to the initial direction toward the target star. Additionally, to simplify the equations we assume that \mathbf{B}_1 is parallel to \mathbf{e}_α and \mathbf{B}_2 is parallel to \mathbf{e}_δ .

2.2. Proper motion, parallax and companions

The proper motion is a projection on the sky of the motion of a star with the velocity \mathbf{V} and within the first order approximation astrometrically only its transverse component $\mathbf{V}_T = V_\alpha \mathbf{e}_\alpha + V_\delta \mathbf{e}_\delta$ is observable. Thus using simple arguments we find that

$$\delta\mathbf{S}_\mu(t) = \pi (V_\alpha t \mathbf{e}_\alpha + V_\delta t \mathbf{e}_\delta) = \cos \delta \mu_\alpha t \mathbf{e}_\alpha + \mu_\delta t \mathbf{e}_\delta, \quad (16)$$

where

$$V_\alpha = \mathbf{V} \cdot \mathbf{e}_\alpha, \quad V_\delta = \mathbf{V} \cdot \mathbf{e}_\delta \quad \text{and} \quad \mu_\alpha = \frac{d\alpha}{dt}(t_0), \quad \mu_\delta = \frac{d\delta}{dt}(t_0). \quad (17)$$

and $\pi = 1/D^*$ where $D^* = \|\mathbf{R}_0\|$ is the SSB distance to the star.

If the star has companions then the proper motion refers to the motion of the mass center of the system and the first order correction due to the orbital is given by the following equation

$$\delta \mathbf{S}_c(t) = \pi [R_\alpha^*(t) \mathbf{e}_\alpha + R_\delta^*(t) \mathbf{e}_\delta], \quad (18)$$

where $\mathbf{R}^* = (R_\alpha^*, R_\delta^*, R_r^*)$ denotes the radius vector of the star with respect to the barycenter of its system in the local frame $\{\mathbf{e}_\alpha, \mathbf{e}_\delta, \mathbf{e}_r\}$.

If the interferometer is located at $\mathbf{R}_O(t)$ in SSB frame then the observed direction toward the star is

$$\mathbf{s}(t) = \mathbf{S}(t) + \mathbf{\Pi}(t), \quad (19)$$

where $\mathbf{\Pi}(t)$ is the parallactic displacement

$$\mathbf{\Pi}(t) = \pi \mathbf{S}_0 \times (\mathbf{S}_0 \times \mathbf{R}_O(t)) \quad (20)$$

obtained from the equation (6) by substituting $-\mathbf{R}_O$ for $\delta \mathbf{R}$. In the local frame the parallactic displacement can be written in the following form

$$\mathbf{\Pi}(t) = \pi [\Pi_\alpha(t) \mathbf{e}_\alpha + \Pi_\delta(t) \mathbf{e}_\delta], \quad (21)$$

where

$$\Pi_\alpha(t) = -\mathbf{R}_O(t) \cdot \mathbf{e}_\alpha = X_O(t) \sin \alpha - Y_O(t) \cos \alpha, \quad (22)$$

$$\Pi_\delta(t) = -\mathbf{R}_O(t) \cdot \mathbf{e}_\delta = X_O(t) \sin \delta \cos \alpha + Y_O(t) \sin \delta \sin \alpha - Z_O(t) \cos \delta \quad (23)$$

and $(X_O(t), Y_O(t), Z_O(t))$ are the coordinates of SSB vector $\mathbf{R}_O(t)$. The expressions for $\mathbf{S}_\mu(t)$, $\mathbf{S}_c(t)$ and $\mathbf{\Pi}(t)$ come directly from the formulae (6), (7) and thus represent a first order approximation with respect to π .

Now, using (3)–(20) and assuming that the measurements have been already corrected for aberration and gravitational lensing we can rewrite the delay equation (1) in the form

$$d = d^0 + d^\mu t + \mathbf{d}^\pi \cdot \mathbf{R}_O(t) + \mathbf{d}^c \cdot \mathbf{R}^*(t) + c + \epsilon, \quad (24)$$

where

$$d^0 = \mathbf{B} \cdot \mathbf{S}_0, \quad d^\mu = \pi \mathbf{B} \cdot \mathbf{V}_T = \mathbf{b} \cdot \boldsymbol{\mu}, \quad \boldsymbol{\mu} = (\mu_\alpha \cos \delta, \mu_\delta), \quad (25)$$

$$\mathbf{b} = (\mathbf{B} \cdot \mathbf{e}_\alpha, \mathbf{B} \cdot \mathbf{e}_\delta), \quad \mathbf{d}^\pi = -\pi [\mathbf{B} - (\mathbf{B} \cdot \mathbf{S}_0) \mathbf{S}_0], \quad (26)$$

$$\mathbf{d}^c = \pi \mathbf{b}, \quad \mathbf{R}^*(t) = (R_\alpha^*(t), R_\delta^*(t)). \quad (27)$$

Using (24) we obtain similar formula for the relative delay

$$D = D^0 + D^\mu t + \mathbf{D}^\pi \cdot \mathbf{R}_O(t) + \mathbf{d}^c \cdot \mathbf{R}^*(t) + \epsilon, \quad (28)$$

where

$$\begin{aligned} D^0 &= \mathbf{B} \cdot (\mathbf{S}_0^1 - \mathbf{S}_0^2), & D^\mu &= \mathbf{B} \cdot (\pi_1 \mathbf{V}_T^1 - \pi_2 \mathbf{V}_T^2), \\ \mathbf{D}^\pi &= [\pi_1 (\mathbf{B} \cdot \mathbf{S}_0^1) \mathbf{S}_0^1 - \pi_2 (\mathbf{B} \cdot \mathbf{S}_0^2) \mathbf{S}_0^2] - (\pi_1 - \pi_2) \mathbf{B}. \end{aligned} \quad (29)$$

where the indices 1, 2 refer to the target and reference star respectively. In the above we assumed that only the target star has companions so as \mathbf{d}^c refers to the local reference frame of the target star. Formula (28) plays the fundamental role in our consideration. It explicitly shows the structure of the observed signal that consists of a dominant linear trend modulated by periodicities due to the motion of the interferometer and the companions of the target star.

According to our assumptions a single observation is done for two orthogonal baseline orientations \mathbf{B}_1 and \mathbf{B}_2 . Thus a single observations is given as a two component vector $\mathbf{D} = (D_1, D_2)$ of the relative delays. Each component D_i has the form (28) where coefficients D_i^0 , D_i^μ , \mathbf{D}_i^π and \mathbf{d}_i^c are calculated with the formulae (29) and $\mathbf{B} = \mathbf{B}_i$, $i = 1, 2$ respectively.

2.3. Second order corrections

The above considerations represent first order approximation which is sufficient for most astrometric measurements. However SIM is expected to deliver unprecedented $1\mu\text{as}$ precision in the narrow-angle mode and thus it is important to understand limitation of the model (29). It can be accomplished by analyzing higher order terms. For the baselines perpendicular to \mathbf{S}_0 , the second order corrections correspond to the term that is responsible for the actual angular displacement (see equation (12)) and we have

$$\|\delta\mathbf{S}^{(2)}\| = \frac{\|\delta\mathbf{R}_\parallel\| \|\delta\mathbf{R}_\perp\|}{\|\mathbf{R}_0\| \|\mathbf{R}_0\|} \leq \left(\frac{\|\delta\mathbf{R}\|}{\|\mathbf{R}_0\|} \right)^2 \quad (30)$$

They can be calculated if we put $\delta\mathbf{R} = -\mathbf{R}_O(t) + \mathbf{R}^*(t) + \mathbf{R}_V(t)$ where $\mathbf{R}_V(t) = \mathbf{V}_T t + \mathbf{V}_R t$. We obtain

$$\begin{aligned} \frac{1}{\pi^2} \delta\mathbf{S}^{(2)} &= -\|\mathbf{R}_O^\parallel(t)\| \mathbf{R}_O^\perp(t) + \|\mathbf{R}_*^\parallel(t)\| \mathbf{R}_\perp^*(t) + \|\mathbf{R}_V^\parallel(t)\| \mathbf{R}_V^\perp(t) + \\ &+ \left(\|\mathbf{R}_O^\parallel(t)\| \mathbf{R}_\perp^*(t) - \|\mathbf{R}_*^\parallel(t)\| \mathbf{R}_O^\perp(t) \right) + \left(\|\mathbf{R}_O^\parallel(t)\| \mathbf{R}_V^\perp(t) - \|\mathbf{R}_V^\parallel(t)\| \mathbf{R}_O^\perp(t) \right) + \\ &+ \left(\|\mathbf{R}_*^\parallel(t)\| \mathbf{R}_V^\perp(t) + \|\mathbf{R}_V^\parallel(t)\| \mathbf{R}_\perp^*(t) \right) \end{aligned} \quad (31)$$

and

$$\begin{aligned} \|\delta\mathbf{S}^{(2)}\| &\leq \pi^2 (\|\mathbf{R}_O(t)\|^2 + \|\mathbf{R}^*(t)\|^2 + \|\mathbf{R}_V(t)\|^2 + \\ &- 2\mathbf{R}_O(t) \cdot \mathbf{R}^*(t) - 2\mathbf{R}_O(t) \cdot \mathbf{R}_V(t) + 2\mathbf{R}^*(t) \cdot \mathbf{R}_V(t)) \end{aligned} \quad (32)$$

As we can see there are two types of second order corrections. The first type includes the second order corrections due to the proper motion, parallax and companions. For the proper motion it is easy to calculate its exact value

$$\Delta S_\mu = \frac{1}{4} \frac{\|\mathbf{V}_T\| \|\mathbf{V}_R\|}{\|\mathbf{R}_O\| \|\mathbf{R}_O\|} \Delta T^2 = \frac{\pi^2}{4} V_T V_R \Delta T^2 \quad (33)$$

where ΔT is the time span of the mission (and we assumed that t_0 is at half of ΔT), $\|\mathbf{V}_T\| = V_T$, $\|\mathbf{V}_R\| = V_R$. In order to learn about the magnitude of this correction, we calculated its value for the sample of 150 stars from the Hipparcos catalogue with the largest proper motion (see the Internet location <http://astro.estec.esa.nl/SA-general/Projects/Hipparcos/hipparcos.html>). The results are shown in Fig. 3. As one can see ΔS_μ is indeed significant for such stars and without any doubts has to be included into the model. For the remaining corrections due to the motion of the interferometer (i.e. the second order parallactic correction) and the presence of a companion we have the following upper limits

$$\begin{aligned} \pi^2 \|\mathbf{R}_O^{\parallel}(t)\| \|\mathbf{R}_O^{\perp}(t)\| &\leq \pi^2 \|\mathbf{R}_O(t)\|^2 \lesssim \Delta S_\pi = \pi^2 a_O^2, \\ \pi^2 \|\mathbf{R}_\star^{\parallel}(t)\| \|\mathbf{R}_\star^{\perp}(t)\| &\leq \pi^2 \|\mathbf{R}^\star(t)\|^2 \lesssim \Delta S_c = \pi^2 (a_\star / (1 - e_\star))^2 \end{aligned} \quad (34)$$

where a_O is SIM's orbit semi-major axis, a_\star semi-major axis of the star's orbit and e_\star its eccentricity. If we assume that SIM semi-major axis is 1 AU then

$$\begin{aligned} \Delta S_c &\approx 5 \times 10^{-6} \frac{m_{MJUP}^2 P_{yr}^{4/3}}{d_{pc}^2 M_{M_\odot}^{4/3} (1 - e)^2} \mu as \quad \text{for planetary companions} \\ \Delta S_c &\approx 4.9 \frac{m_{M_\odot}^2 P_{yr}^{4/3}}{d_{pc}^2 M_{M_\odot}^{4/3} (1 + m_{M_\odot}/M_{M_\odot})^{4/3} (1 - e)^2} \mu as \quad \text{for stellar companions} \\ \Delta S_\pi &\approx 4.9 d_{pc}^{-2} \mu as \end{aligned} \quad (35)$$

where d_{pc} is the distance to the star in parsecs, M_{M_\odot} mass of the star in solar masses, m_{M_\odot} mass of the companion in solar masses, m_{MJUP} mass of the companion in Jupiter masses, P_{yr} orbital period in years and e eccentricity.

The other type of second order corrections includes all "mixed" terms

$$\begin{aligned} \pi^2 \|\|\mathbf{R}_O^{\parallel}(t)\| \|\mathbf{R}_\star^{\perp}(t)\| - \|\mathbf{R}_\star^{\parallel}(t)\| \|\mathbf{R}_O^{\perp}(t)\|\| &\leq 2\pi^2 |\mathbf{R}_O(t) \cdot \mathbf{R}^\star(t)| \lesssim \Delta \Pi_c = 2\pi^2 a_O a_\star / (1 - e_\star), \\ \pi^2 \|\|\mathbf{R}_\star^{\parallel}(t)\| \|\mathbf{R}_V^{\perp}(t)\| + \|\mathbf{R}_V^{\parallel}(t)\| \|\mathbf{R}_\star^{\perp}(t)\|\| &\leq 2\pi^2 |\mathbf{R}^\star(t) \cdot \mathbf{R}_V(t)| \lesssim \Delta \Psi_c = \pi^2 V \Delta T a_\star / (1 - e_\star), \end{aligned} \quad (36)$$

$$\pi^2 \|\|\mathbf{R}_O^{\parallel}(t)\| \|\mathbf{R}_V^{\perp}(t)\| - \|\mathbf{R}_V^{\parallel}(t)\| \|\mathbf{R}_O^{\perp}(t)\|\| \leq 2\pi^2 |\mathbf{R}_O(t) \cdot \mathbf{R}_V(t)| \lesssim \Delta \Pi_\mu = \pi^2 a_O V \Delta T$$

where $V = (V_T^2 + V_R^2)^{1/2}$. The value of $\Delta \Pi_\mu$ has been calculated for the same sample of stars as in Fig. 3. Again, one can observe that $\Delta \Pi_\mu$ is significant and a proper model has to take it into

account (see Fig. 4). We also find that

$$\begin{aligned} \Delta\Pi_c &\approx 9 \times 10^{-3} \frac{m_{MJUP} P_{yr}^{2/3}}{d_{pc}^2 M_{M_\odot}^{2/3} (1-e)} \mu as \quad \text{for planetary companions} \\ \Delta\Pi_c &\approx 9.7 \frac{m_{M_\odot} P_{yr}^{2/3}}{d_{pc}^2 M_{M_\odot}^{2/3} (1+m_{M_\odot}/M_{M_\odot})^{2/3} (1-e)} \mu as \quad \text{for stellar companions} \end{aligned} \quad (37)$$

and

$$\begin{aligned} \Delta\Psi_c &\approx 0.1 V_{100} \Delta T_{yr} \frac{m_{MJUP} P_{yr}^{2/3}}{d_{pc}^2 M_{M_\odot}^{2/3} (1-e)} \mu as \quad \text{for planetary companions} \\ \Delta\Psi_c &\approx 102.3 V_{100} \Delta T_{yr} \frac{m_{M_\odot} P_{yr}^{2/3}}{d_{pc}^2 M_{M_\odot}^{2/3} (1+m_{M_\odot}/M_{M_\odot})^{2/3} (1-e)} \mu as \quad \text{for stellar companions} \end{aligned} \quad (38)$$

where V_{100} is the velocity of star in hundreds of km/s and ΔT_{yr} is the time span of the mission in years.

Finally, let us shortly discuss the magnitude of third order terms. Obviously, they will be detectable only for $\delta\mathbf{R}$ due to the proper motion. Thus we can estimate that the resulting angular displacement $\delta S^{(3)}$ is

$$\delta S^{(3)} \sim \left(\frac{\|\delta\mathbf{R}\|}{\|\mathbf{R}_0\|} \right)^3 = \frac{\pi^3}{8} V^3 \Delta T^3 = \frac{\pi^3}{8} (V_R^2 + V_T^2)^{3/2} \Delta T^3 \quad (39)$$

Its value for the sample of stars from Figs. 3-4 is presented in Fig. 5. As one can see in few cases this third order term can be larger than $1\mu as$.

The above analysis clearly shows that a variety of second order effects and possibly in few cases third order effects will be detectable with SIM. Although throughout the rest of this paper we use only the first order model presented in sections 2.1-2 to simplify our considerations, in real applications a correct model must include higher order effects. They can be easily derived given the theoretical background presented in section 2.

3. Orbital motion

Let us assume that the motion of N planets and their star is described in the barycentric system. From the definition of such system, we have the following relation for the radius vector of the parent star

$$\mathbf{R}^* = -\frac{1}{M_\star} \sum_{j=1}^N m_j \mathbf{R}_j, \quad (40)$$

where \mathbf{R}_j are radius vectors of planets and M_* , m_j are the mass of the star and the j -th planet, respectively. In the first approximation, the motion of planets can be described by means of the following equations

$$\frac{d^2 \mathbf{R}_j}{dt^2} = -\mu_j \frac{\mathbf{R}_j}{\|\mathbf{R}_j\|^3}, \quad j = 1, \dots, N, \quad (41)$$

where

$$\mu_j = \frac{GM_*}{(1 + m_j/M_*)^2}.$$

and the motion of the star can be obtained from the equation (40).

3.1. Elliptic motion and its expansion

Solutions $\mathbf{R}_j(t)$ of the equations (41) belong to the family of Keplerian orbits among which elliptic orbits are of particular interest for farther analysis. Therefore, let us remind their basic properties.

The radius vector $\mathbf{R}_j = \mathbf{R}(t)$ of a planet moving in an elliptic orbit is given by

$$\mathbf{R}(t) = \mathbf{P} a(\cos E(t) - e) + \mathbf{Q} a\sqrt{1 - e^2} \sin E(t), \quad (42)$$

where

$$\mathbf{P} = \mathbf{l} \cos \omega + \mathbf{m} \sin \omega, \quad \mathbf{Q} = -\mathbf{l} \sin \omega + \mathbf{m} \cos \omega,$$

$$\mathbf{l} = \begin{bmatrix} \cos \Omega \\ \sin \Omega \\ 0 \end{bmatrix}, \quad \mathbf{m} = \begin{bmatrix} -\cos i \sin \Omega \\ \cos i \cos \Omega \\ \sin i \end{bmatrix}.$$

The eccentric anomaly $E = E(t)$ is an implicit function of time through the Kepler equation

$$E - e \sin E = \mathcal{M}, \quad (43)$$

where \mathcal{M} is the mean anomaly

$$\mathcal{M} = n(t - T_p), \quad n = \frac{2\pi}{P}, \quad (44)$$

and P is the orbital period of a planet. The remaining parameters $a, e, \omega, \Omega, T_p$ are the standard Keplerian elements — semi-major axis, eccentricity, longitude of pericenter, longitude of ascending node and time of pericenter.

The functions $\cos E$ and $\sin E$ are periodic with respect to \mathcal{M} and can be expanded in the Fourier series

$$\begin{aligned}\cos E &= -\frac{1}{2}e + \sum_{k \in \mathcal{Z}_0} \frac{1}{k} J_{k-1}(ke) \cos(k\mathcal{M}), \\ \sin E &= \sum_{k \in \mathcal{Z}_0} \frac{1}{k} J_{k-1}(ke) \sin(k\mathcal{M}),\end{aligned}\tag{45}$$

where $J_n(z)$ is a Bessel function of the first kind of order n and argument z ; \mathcal{Z}_0 denotes the set of all positive and negative integers excluding zero, and $e \in [0, 1)$. Thus, using the equations (42) and (45), we obtain

$$\widehat{\mathbf{R}}(t) = \widehat{\mathbf{R}}^0 + \mathbf{A} \sum_{k \in \mathcal{Z}_0} \frac{1}{k} J_{k-1}(ke) \cos(k\mathcal{M}) + \mathbf{B} \sum_{k \in \mathcal{Z}_0} \frac{1}{k} J_{k-1}(ke) \sin(k\mathcal{M}),\tag{46}$$

where

$$\widehat{\mathbf{R}}(t) = \frac{1}{a}\mathbf{R}, \quad \widehat{\mathbf{R}}^0 = -\frac{3}{2}\mathbf{P}e, \quad \mathbf{A} = \mathbf{P} \quad \mathbf{B} = \mathbf{Q}\sqrt{1-e^2}.$$

It can be written in the following complex form

$$\widehat{\mathbf{R}}(t) = \widehat{\mathbf{R}}^0 + \sum_{k \in \mathcal{Z}_0} \boldsymbol{\Theta}_k e^{ik\mathcal{M}},\tag{47}$$

where

$$\boldsymbol{\Theta}_k = \frac{1}{2k} (F_-(k, e)\mathbf{A} - iF_+(k, e)\mathbf{B}),\tag{48}$$

and

$$F_{\pm}(k, e) = J_{k-1}(ke) \pm J_{k+1}(ke).\tag{49}$$

Eventually, using (44) and (47), we obtain the Fourier expansion of $\widehat{\mathbf{R}}(t)$

$$\widehat{\mathbf{R}}(t) = \widehat{\mathbf{R}}^0 + \sum_{k \in \mathcal{Z}_0} \boldsymbol{\Lambda}_k e^{iknt}, \quad \text{where } \boldsymbol{\Lambda}_k = \boldsymbol{\Theta}_k e^{-iknT_{\mathbb{P}}}.\tag{50}$$

Let us define the following quantity

$$\mathcal{A}_k^l = \frac{|\Lambda_{k+1}^l|}{|\Lambda_k^l|}, \quad \text{for } l = 1, 2, 3, \quad \text{and } k > 0,\tag{51}$$

i.e. the ratio of amplitudes of two successive harmonics, where Λ_j^i is the i -th component of vector $\boldsymbol{\Lambda}_j$. From the properties of Bessel functions we have

$$\mathcal{A}_k^l(e) = \frac{k}{k+1} \sqrt{\frac{e^2(A^l)^2 [J'_{k+1}((k+1)e)]^2 + (B^l)^2 [J_{k+1}((k+1)e)]^2}{e^2(A^l)^2 [J'_k(ke)]^2 + (B^l)^2 [J_k(ke)]^2}},\tag{52}$$

where $J'_n(z)$ indicates the derivative of a Bessel function $J_n(z)$ with respect to z . It can be proved that for all $e \in (0, 1)$, $l \in \{1, 2, 3\}$ and $k > 0$ we have $\mathcal{A}_k^l(e) < 1$. It means that the expansion of $\widehat{\mathbf{R}}(t)$ has an important property—moduli of successive harmonics of each of coordinates of $\widehat{\mathbf{R}}(t)$ decrease strictly monotonically with k .

3.2. Real expansion

Given the equations from the previous section, it is possible to derive the real expansion for every component of the vector $\widehat{\mathbf{R}}(t) = (\widehat{R}_1(t), \widehat{R}_2(t), \widehat{R}_3(t))$. Namely, we can express this vector in the form

$$\widehat{\mathbf{R}}(t) = \widehat{\mathbf{R}}^0 + \sum_{k=1}^{\infty} \left(\mathbf{C}^k \cos(knt) + \mathbf{S}^k \sin(knt) \right) \quad (53)$$

which is more convenient in numerical applications. Using (47), (48) and (50) we find

$$\begin{aligned} \mathbf{C}^k &= \frac{1}{k} \left[\mathbf{P}F_-(k, e) \cos(knT_p) - \mathbf{Q}\sqrt{1-e^2}F_+(k, e) \sin(knT_p) \right], \\ \mathbf{S}^k &= \frac{1}{k} \left[\mathbf{P}F_-(k, e) \sin(knT_p) + \mathbf{Q}\sqrt{1-e^2}F_+(k, e) \cos(knT_p) \right]. \end{aligned} \quad (54)$$

From the above formulae immediately follows that amplitudes of successive harmonics are given by

$$(D_l^k)^2 = (C_l^k)^2 + (S_l^k)^2 = \frac{1}{k^2} [P_l^2 F_-(k, e)^2 + Q_l^2 (1 - e^2) F_+(k, e)^2], \quad l = 1, 2, 3. \quad (55)$$

In applications it is convenient to have these expressions in an explicit form

$$\begin{aligned} (D_1^k)^2 &= \frac{1}{k^2} \left[F_-(k, e)^2 (1 - \sin^2 i \sin^2 \Omega) + F(k, e) (\cos \Omega \sin \omega + \cos i \sin \Omega \cos \omega)^2 \right] \\ (D_2^k)^2 &= \frac{1}{k^2} \left[F_-(k, e)^2 (1 - \sin^2 i \cos^2 \Omega) + F(k, e) (\sin \Omega \sin \omega - \cos i \cos \Omega \cos \omega)^2 \right] \\ (D_3^k)^2 &= \frac{1}{k^2} [F_-(k, e)^2 + F(k, e) \cos^2 \omega] \sin^2 i, \end{aligned} \quad (56)$$

where

$$F(k, e) = (1 - e^2)F_+(k, e)^2 - F_-(k, e)^2.$$

3.3. Approximate formulae for small and moderate eccentricities

Since small and moderate eccentricities are more probable it is useful to have approximations of the expressions from the previous section. Namely, using known expansions for Bessel functions we obtain the following formulae

$$F_{\pm}(k, e) = \frac{1}{(k-1)!} \left(\frac{ke}{2} \right)^{k-1} + \mathcal{O}(e^{k+1}), \quad \sqrt{1-e^2}F_+(k, e) = \frac{1}{(k-1)!} \left(\frac{ke}{2} \right)^{k-1} + \mathcal{O}(e^{k+1}) \quad (57)$$

Subsequently

$$\begin{aligned} \mathbf{C}^k &= \frac{1}{k(k-1)!} \left(\frac{ke}{2} \right)^{k-1} [\mathbf{1} \cos \tilde{\omega}_k + \mathbf{m} \sin \tilde{\omega}_k] + \mathcal{O}(e^{k+1}), \\ \mathbf{S}^k &= \frac{1}{k(k-1)!} \left(\frac{ke}{2} \right)^{k-1} [-\mathbf{1} \sin \tilde{\omega}_k + \mathbf{m} \cos \tilde{\omega}_k] + \mathcal{O}(e^{k+1}). \end{aligned} \quad (58)$$

where $\tilde{\omega}_k = \omega - knT_p$. Finally, we obtain the expansions for the amplitudes

$$\begin{aligned}
 (D_1^k)^2 &= \left[\frac{1}{k(k-1)!} \left(\frac{ke}{2} \right)^{k-1} \right]^2 (1 - \sin^2 i \sin^2 \Omega) + \mathcal{O}(e^{2k}), \\
 (D_2^k)^2 &= \left[\frac{1}{k(k-1)!} \left(\frac{ke}{2} \right)^{k-1} \right]^2 (1 - \sin^2 i \cos^2 \Omega) + \mathcal{O}(e^{2k}), \\
 (D_3^k)^2 &= \left[\frac{1}{k(k-1)!} \left(\frac{ke}{2} \right)^{k-1} \right]^2 \sin^2 i + \mathcal{O}(e^{2k}).
 \end{aligned} \tag{59}$$

From the above we can obtain the harmonic expansion for a circular orbit. Namely we find that $\hat{\mathbf{R}}^0 = \mathbf{0}$ and $\mathbf{C}^k = \mathbf{S}^k = \mathbf{0}$ for $k > 1$. While for $k = 1$

$$\begin{aligned}
 \mathbf{C}^k &= [\mathbf{1} \cos \tilde{\omega} + \mathbf{m} \sin \tilde{\omega}], \\
 \mathbf{S}^k &= [-\mathbf{1} \sin \tilde{\omega} + \mathbf{m} \cos \tilde{\omega}].
 \end{aligned} \tag{60}$$

where $\tilde{\omega} = -nT_p$.

These equations will be especially useful for deriving orbital elements from the coefficients $\mathbf{C}^k, \mathbf{S}^k$ obtained through the analysis of observations. We discuss this issue in the next section.

4. Data analysis

For the tests we assume the following SIM observing scenario. At the moments t_i and t_{i+1} the relative delay between the target and reference star is measured for two orthogonal baseline orientations \mathbf{B}_1 and \mathbf{B}_2 . Such measurement gives a two dimensional delay vector $\mathbf{D}_i = (D_1(t_i), D_2(t_{i+1}))$ and is repeated N times over the time span of the mission, ΔT . As a result we obtain a two dimensional time series $\mathcal{D} = \{\mathbf{D}_i, i = 1, \dots, N\}$. The goal of the data analysis is to detect planetary signatures in \mathcal{D} and derive the orbital parameters of planets. We solve this problem in two steps. First we perform Frequency Decomposition (FD) of the time series \mathcal{D} . The aim of this step is to understand the basic properties of \mathcal{D} i.e. determine the number of planets and estimate their orbital parameters. The second step is the least-squares analysis based on a specific physical model established in the previous step. Its aim is to obtain accurate values of the orbital elements and their uncertainties. These two steps are described in the following sections.

4.1. Harmonic model

From the theoretical considerations of sections 2 and 3 it follows that relative delays can be modeled by means of the following expression

$$\begin{aligned} \mathbf{D} = & \widehat{\mathbf{D}}^0 + \widehat{\mathbf{D}}^\mu t + \sum_{k=1}^{\infty} \left[\widehat{\mathbf{C}}^{\pi,k} \cos(n_O kt) + \widehat{\mathbf{S}}^{\pi,k} \cos(n_O kt) \right] + \\ & + \sum_{j=1}^N \sum_{k=1}^{\infty} \left[\widehat{\mathbf{C}}^{j,k} \cos(n_j kt) + \widehat{\mathbf{S}}^{j,k} \cos(n_j kt) \right], \end{aligned} \quad (61)$$

where N denotes the number of planets, n_O and n_j denote the mean motion of SIM and j -th planet, respectively. Such equation comes directly from the fact that the motion of the interferometer and the motion of planets can be expanded into the Fourier series. Consequently, the above formula is used to describe \mathcal{D} and special numerical algorithm is used to obtain the parameters

$$\widehat{\mathbf{D}}^0 = \begin{bmatrix} \widehat{D}_1^0 \\ \widehat{D}_2^0 \end{bmatrix}, \quad \widehat{\mathbf{D}}^\mu = \begin{bmatrix} \widehat{D}_1^\mu \\ \widehat{D}_2^\mu \end{bmatrix}, \quad \widehat{\mathbf{C}}^{\pi,k} = \begin{bmatrix} \widehat{C}_1^{\pi,k} \\ \widehat{C}_2^{\pi,k} \end{bmatrix}, \quad \widehat{\mathbf{S}}^{\pi,k} = \begin{bmatrix} \widehat{S}_1^{\pi,k} \\ \widehat{S}_2^{\pi,k} \end{bmatrix}, \quad (62)$$

$$\widehat{\mathbf{C}}^{j,k} = \begin{bmatrix} \widehat{C}_1^{j,k} \\ \widehat{C}_2^{j,k} \end{bmatrix}, \quad \widehat{\mathbf{S}}^{j,k} = \begin{bmatrix} \widehat{S}_1^{j,k} \\ \widehat{S}_2^{j,k} \end{bmatrix}, \quad n_j, \quad n_O, \quad j = 1, \dots, N, \quad k = 1, \dots, K_j,$$

This algorithm has been described in great detail in Konacki, Maciejewski & Wolszczan (1999). Let us only note here that in practice, due to limited accuracy of measurements and the fact that the amplitudes of subsequent harmonics decrease monotonically, the expansions of (61) are finite and the (finite) number of harmonics K_j depends mainly on orbital eccentricities and measurement errors. Using our algorithm we can determine the number of planets N , the number of detectable harmonics K_j and determine the basic frequencies and coefficients of (61).

In fact, we can assume that the mean motion of SIM n_O as well as the other elements of its orbit are known. In other words $\mathbf{R}_O(t)$ is known and we can use the following more constrained version of the formula (61)

$$\mathbf{D} = \widehat{\mathbf{D}}^0 + \widehat{\mathbf{D}}^\mu t + \widehat{\mathbb{D}}^\pi \cdot \mathbf{R}_O(t) + \sum_{j=1}^N \sum_{k=1}^{K_j} \left[\widehat{\mathbf{C}}^{j,k} \cos(n_j kt) + \widehat{\mathbf{S}}^{j,k} \cos(n_j kt) \right], \quad (63)$$

This way instead of several parameters $\widehat{\mathbf{C}}^{\pi,k}, \widehat{\mathbf{S}}^{\pi,k}, n_O$ we have six parameters since

$$\widehat{\mathbb{D}}^\pi = \begin{bmatrix} \widehat{D}_{11}^\pi, \widehat{D}_{12}^\pi, \widehat{D}_{13}^\pi \\ \widehat{D}_{21}^\pi, \widehat{D}_{22}^\pi, \widehat{D}_{23}^\pi \end{bmatrix} \quad (64)$$

In order to have a better understanding of the parameters of (63) let us express them by means

of the quantities introduced in section 2. Using (28), (29) and (50) we find that

$$\begin{aligned}\widehat{\mathbf{D}}^0 &= \begin{bmatrix} \widehat{D}_1^0 \\ \widehat{D}_2^0 \end{bmatrix} = \begin{bmatrix} D_1^0 \\ D_2^0 \end{bmatrix} - \pi_1 \sum_{j=1}^N \frac{m_j}{M_\star} a_j \begin{bmatrix} B_1 \widehat{R}_1^{0,j} \\ B_2 \widehat{R}_2^{0,j} \end{bmatrix}, \\ \widehat{\mathbf{D}}^\mu &= \begin{bmatrix} \widehat{D}_1^\mu \\ \widehat{D}_2^\mu \end{bmatrix} = \begin{bmatrix} D_1^\mu \\ D_2^\mu \end{bmatrix}, \quad \widehat{\mathbb{D}}^\pi = \begin{bmatrix} \widehat{D}_{11}^\pi, \widehat{D}_{12}^\pi, \widehat{D}_{13}^\pi \\ \widehat{D}_{21}^\pi, \widehat{D}_{22}^\pi, \widehat{D}_{23}^\pi \end{bmatrix} = \begin{bmatrix} \mathbf{D}_1^\pi \\ \mathbf{D}_2^\pi \end{bmatrix}\end{aligned}\tag{65}$$

where D_i^0 , D_i^μ and \mathbf{D}_i^π are the quantities defined by (29) and calculated for $\mathbf{B} = \mathbf{B}_i$, $i = 1, 2$; $\widehat{\mathbf{R}}^{0,j}$ denotes $\widehat{\mathbf{R}}^0$ in the expansion (53) for the orbit of the j -th planet and a_j is the semi-major axis of the j -th planet. The coordinates of $\widehat{\mathbf{R}}^j = (\widehat{R}_1^j, \widehat{R}_2^j, \widehat{R}_3^j)$ are expressed in the local frame $\{\mathbf{e}_\alpha, \mathbf{e}_\delta, \mathbf{e}_r\}$. This way

$$\begin{aligned}\mathbf{d}^c \cdot \widehat{\mathbf{R}}^j &= \pi_1 (\mathbf{B}_1 \cdot \mathbf{e}_\alpha) \widehat{R}_1^j = \pi_1 B_1 \widehat{R}_1^j, \quad \text{for } \mathbf{B}_1 \\ \mathbf{d}^c \cdot \mathbf{R}^j &= \pi_1 (\mathbf{B}_2 \cdot \mathbf{e}_\delta) \widehat{R}_2^j = \pi_1 B_2 \widehat{R}_2^j, \quad \text{for } \mathbf{B}_2\end{aligned}\tag{66}$$

since $\mathbf{B}_1 = B_1 \mathbf{e}_\alpha$, $\mathbf{B}_2 = B_2 \mathbf{e}_\delta$ where B_i is the length of the baseline vector \mathbf{B}_i . Similarly we have

$$\widehat{\mathbf{C}}^{j,k} = -\pi_1 \frac{m_j}{M_\star} a_j \begin{bmatrix} B_1 C_1^{j,k} \\ B_2 C_2^{j,k} \end{bmatrix}, \quad \widehat{\mathbf{S}}^{j,k} = -\pi_1 \frac{m_j}{M_\star} a_j \begin{bmatrix} B_1 S_1^{j,k} \\ B_2 S_2^{j,k} \end{bmatrix},\tag{67}$$

where $\mathbf{C}^{j,k} = (C_1^{j,k}, C_2^{j,k}, C_3^{j,k})$ and $\mathbf{S}^{j,k} = (S_1^{j,k}, S_2^{j,k}, S_3^{j,k})$ are \mathbf{C}^k and \mathbf{S}^k coefficients of expansion (53) for j -th planet expressed in the local frame.

Now let us assume that after performing FD, we obtained the parameters

$$\widehat{\mathbf{D}}^0, \quad \widehat{\mathbf{D}}^\mu, \quad \widehat{\mathbb{D}}^\pi, \quad \widehat{\mathbf{C}}^{j,k}, \quad \widehat{\mathbf{S}}^{j,k}, \quad j = 1, \dots, N, \quad k = 1, \dots, K_j\tag{68}$$

where N is the number of planets (i.e. the number of basic frequencies detected) and K_j is the number of detected harmonics for each planet. The first question is if we can derive the canonical parameters like $\alpha, \delta, \mu_\alpha, \mu_\delta, \pi$ for the target and reference star from $\widehat{\mathbf{D}}^0, \widehat{\mathbf{D}}^\mu, \widehat{\mathbb{D}}^\pi$. Unfortunately this is not possible, at least without additional assumptions. Obviously it is a direct consequence of the relative measurements we perform. Thus we can only derive $(\mathbf{S}_0^1 - \mathbf{S}_0^2)$ as well as differential proper motion and differential parallax. In fact it is possible to chose such a reference star that the differential parallactic displacement has an amplitude close to zero. It suffice to have a reference star with the parallax similar to the parallax of the target star since by assumption these two stars are close to each other and their parallactic displacement is very similar. This way we can remove a strong parallactic component from our observations. On the other hand we do not need the exact values of the canonical parameters. We only have to properly remove the respective effects in order to be able to detect putative planets.

The remaining question is if we can derive the orbital elements from $\widehat{\mathbf{C}}^{j,k}, \widehat{\mathbf{S}}^{j,k}$. This task is relatively simple. Namely, given that we have detected at least two terms (basic frequency and its

first harmonics), all orbital elements can be derived from the equations of section 3.3. For planets with only the basic frequency detectable, we assume a circular orbit and then the other elements can also be found. This procedure we demonstrate in section 5.

4.2. Standard model

The harmonic model allows us to describe the data without a priori knowledge of the target star parameters and its planetary system. In the same time it allows to derive all important information — especially the number of planets and estimates of their orbital elements. With such knowledge we are ready to perform the standard least-squares analysis in which we must specify the model and supply good initial conditions for the fit.

The standard model has the following form

$$\mathbf{D} = \widehat{\mathbf{D}}^0 + \widehat{\mathbf{D}}^\mu t + \widehat{\mathbb{D}}^\pi \cdot \mathbf{R}_O(t) + \sum_{j=1}^N \begin{bmatrix} \widehat{a}_j B_1 \widehat{R}_1(t, T_{p,j}, e_j, i_j, \omega_j, \Omega_j, P_j) \\ \widehat{a}_j B_2 \widehat{R}_2(t, T_{p,j}, e_j, i_j, \omega_j, \Omega_j, P_j) \end{bmatrix}, \quad (69)$$

where $\widehat{R}_1, \widehat{R}_2$ are coordinates of the Keplerian motion vector $\widehat{\mathbf{R}}$ given by the equation (46). The parameters of such model are

$$\mathbf{D}^0, \quad \mathbf{D}^\mu, \quad \mathbb{D}^\pi, \quad \widehat{a}_j, T_{p,j}, e_j, i_j, \omega_j, \Omega_j, P_j, \quad j = 1, \dots, N, \quad (70)$$

where $T_{p,j}, e_j, i_j, \omega_j, \Omega_j$ are the Keplerian elements of the j -th planet, P_j is its orbital period and the parameter \widehat{a}_j is defined in the following way

$$\widehat{a}_j = \pi_1 a_j \frac{m_j}{M_\star} \quad (71)$$

5. Numerical tests

For the tests we chose ν And with its two outer planets (Butler et al. 1999). All real and assumed astrometric and orbital parameters are presented in Table 1. We also found a reference star HD 10032 which is about 0.7° away from ν And. Its astrometric parameters are in Table 2. SIM is assumed to move in an orbit similar to the orbit of the Earth (see Table 3). For these stars we simulated $N = 200$ measurements of relative delays (D_1, D_2) (for two baseline vector orientations \mathbf{B}_1 and \mathbf{B}_2) randomly distributed over the time span of 10 years. In both cases the length of the baseline vector was 10 meters and a measurement error with $\sigma \approx 50$ pm was assumed (i.e. $1\mu as$ in angular displacement). Since by assumption \mathbf{B}_1 is parallel to \mathbf{e}_α and \mathbf{B}_2 to \mathbf{e}_δ , the delay D_1 corresponds to an angular distance between ν And and HD 10032 in right ascension and D_2 to an angular distance in declination.

5.1. Second order effects

Before we proceed with the analysis it is interesting to discuss second order effects present in simulated observations. Since ν And is a nearby star with large proper motion we can expect significant contribution from this star (our reference star HD 10032 is quite distant and thus all second order effects are mainly due to ν And). One can analyze these effects by means of the formulae from section 2.3 or simply apply the standard model (69) with the parameters precisely computed from assumed parameters of ν And, HD 10032 and SIM (Tables 1-3) and examine the resulting residuals. This procedure gives the residuals presented in Fig. 6. As we can see the second order effects are dominated by a variation quadratic in time (Fig. 6 a,b). This effect is due to perspective acceleration

$$\frac{\pi^2}{4} \|\mathbf{V}_R\| \|\mathbf{V}_T\| \Delta T^2 \quad (72)$$

thus if we assume that the radial velocity, \mathbf{V}_R , of ν And and HD 10032 is zero it will disappear and reveal another second order effect of smaller magnitude (see Fig. 6 c,d). This effect is due to the following term

$$\pi^2 \|\mathbf{R}_O^\parallel(t)\| \|\mathbf{R}_V^\perp(t)\| - \pi^2 \|\mathbf{R}_V^\parallel(t)\| \|\mathbf{R}_O^\perp(t)\| \quad (73)$$

i.e. the mixed term of parallax and motion of the star.

Finally let us note that if we allow the parameters of the model (69) to vary, as usual during the process of least-squares fit, this first order model will try to minimize the residuals as presented in Fig. 6 e,f.

5.2. Frequency Decomposition and standard model

First step in our analysis of simulated relative delay measurements is the Frequency Decomposition (FD). Here we model the data with the less constrained formula (61) to show how the parallactic motion contributes to the data. From assumed parameters of the stars and SIM we can compute amplitudes of basic terms and their harmonics. They are shown in Fig. 7. The main idea of FD is subsequent removal of effects with decreasing magnitudes (for all details of the method see Konacki, Maciejewski & Wolszczan (1999)). This process is demonstrated in Fig. 8 and 9 for D_1 (i.e. for delays measured with the baseline vector orientation \mathbf{B}_1). As one can see the most significant part of delay variations comes from the proper motion of both stars (Fig. 8a), then we can detect the basic term of the parallactic motion (Fig. 8b), the basic term of the planet II (Fig. 8c), first harmonic of the parallactic motion (Fig. 8d), the basic term of the planet I (Fig. 9e), first harmonic of the planet II (Fig. 9f), second harmonic of the planet II (Fig. 9g) and finally first harmonic of the planet I (Fig. 9h). The values of respective parameters $\widehat{\mathbf{S}}^{j,k}$, $\widehat{\mathbf{C}}^{j,k}$ are presented in Table 4. They are sufficient to derive initial estimates of the orbital elements of planets I and II.

Namely, from the approximate equations of section 3.3 we can find that

$$\begin{aligned}
 e_j &= 2 \sqrt{\frac{(\widehat{C}_1^{j,2})^2 + (\widehat{S}_1^{j,2})^2}{(\widehat{C}_1^{j,1})^2 + (\widehat{S}_1^{j,1})^2}}, \\
 \frac{\widehat{S}_1^{j,1}}{B_1} \frac{\widehat{C}_2^{j,1}}{B_2} - \frac{\widehat{S}_2^{j,1}}{B_2} \frac{\widehat{C}_1^{j,1}}{B_1} &= -\widehat{a}_j^2 \cos i_j \\
 \left(\frac{\widehat{C}_1^{j,1}}{B_1}\right)^2 + \left(\frac{\widehat{C}_2^{j,1}}{B_2}\right)^2 - \left(\frac{\widehat{S}_1^{j,1}}{B_1}\right)^2 - \left(\frac{\widehat{S}_2^{j,1}}{B_2}\right)^2 &= \widehat{a}_j^2 \cos 2\tilde{\omega}_{1,j} \sin^2 i_j, \\
 \left(\frac{\widehat{S}_1^{j,1}}{B_1}\right)^2 + \left(\frac{\widehat{C}_1^{j,1}}{B_1}\right)^2 - \left(\frac{\widehat{S}_2^{j,1}}{B_2}\right)^2 - \left(\frac{\widehat{C}_2^{j,1}}{B_2}\right)^2 &= \widehat{a}_j^2 \cos 2\Omega_j \sin^2 i_j, \\
 \frac{\widehat{C}_1^{j,1}}{B_1} \frac{\widehat{S}_1^{j,1}}{B_1} + \frac{\widehat{C}_2^{j,1}}{B_2} \frac{\widehat{S}_2^{j,1}}{B_2} &= -\widehat{a}_j^2 \sin \tilde{\omega}_{1,j} \cos \tilde{\omega}_{1,j} \sin^2 i_j, \\
 \frac{\widehat{C}_1^{j,1}}{B_1} \frac{\widehat{C}_2^{j,1}}{B_2} + \frac{\widehat{S}_1^{j,1}}{B_1} \frac{\widehat{S}_2^{j,1}}{B_2} &= \widehat{a}_j^2 \sin \Omega_j \cos \Omega_j \sin^2 i_j
 \end{aligned} \tag{74}$$

and, together with analogous formulae for first harmonics, easily determine the orbital elements. They are show in Table 5. As one can see this procedure gives quite accurate values of the orbital elements. However we use them only as initial values for the least-squares fit with the standard model (69) to obtain the final parameters presented in Table 6.

5.3. Conclusions

The above test demonstrates that our approach allows us to determine the orbital elements with high confidence, at least in this particular case. It is interesting to note that with FD we are able to estimate the orbital elements without using the entire information present in the simulated data set (the residuals from Fig. 9h are well above the assumed measurement error). Surprisingly this estimation is quite accurate and as demonstrated is perfectly sufficient as an initial guess of the parameters for the standard least-squares analysis. This is a very promising result since the difficult problem of good initial condition is usually solved by means of quasi-global techniques which are very demanding numerically and still may lead to unreliable results. Thus we believe that our approach constitutes safe and efficient solution to the problem of planets detection with SIM. In our forthcoming paper we will thoroughly analyze the method on more realistic simulations and a variety of different planetary systems.

REFERENCES

- Konacki, M. , Maciejewski, A. J. & Wolszczan, A. 1999, *ApJ*, 513, 471
- Konacki, M. and Maciejewski, A. J. 1999, *ApJ*, 518, 442
- Konacki, M. and Maciejewski, A. J. 1999, *Planets Outside the Solar System: Theory and Observations*, NATO Science Series C, (J.-M. Mariotti and D. Alloin, editors), 532, p. 249
- Shao, M. & Baron, R. 1999, *Working on the Fringe: An International Conference on Optical and IR Interferometry from Ground and Space*, ASP Conference Series (S. Unwin and R. Stachnik, editors), 194, p. 107.
- Butler, R. P., Marcy, G. W., Fischer, D. A., Brown, T. M., Contos, A. R., Korzennik, S. G., Nisenson, P. and Noyes, R. W. 1999, *ApJ*, 526, 916

Fig. 1.— Solar System Barycenter (SSB) reference frame and the celestial sphere. \mathbf{S}_0 is the unit vector toward the star with spherical coordinates (α, δ) and $\|\mathbf{R}_0\|$ is the distance to the star.

Fig. 2.— Tangent space at \mathbf{S}_0 where \mathbf{e}_α , \mathbf{e}_δ and \mathbf{e}_r are the unit vectors of the local frame.

Fig. 3.— ΔS_μ for 150 stars with the largest proper motion from the Hipparcos catalogue. The solid lines represent ΔS_μ for 1, 10 and 100 parsecs as a function of $V_T V_R$. Time span of the mission $\Delta T = 10yr$ was assumed.

Fig. 4.— $\Delta \Pi_\mu$ for 150 stars with the largest proper motion from the Hipparcos catalogue. The solid lines represent $\Delta \Pi_\mu$ for 1, 10 and 100 parsecs as a function of V . Time span of the mission $\Delta T = 10yr$ was assumed.

Fig. 5.— $\Delta S^{(3)}$ for 150 stars with the largest proper motion from the Hipparcos catalogue. The solid lines represent $\Delta S^{(3)}$ for 1, 10 and 100 parsecs as a function of V . Time span of the mission $\Delta T = 10yr$ was assumed.

Fig. 6.— Second order effects in the simulated delays for the relative measurements between ν And and HD 10032 for the baseline vector orientations \mathbf{B}_1 (a) and \mathbf{B}_2 (b); (c,d) the same effects when the radial velocity of both stars is zero; (e,f) the residuals from the least-squares fit of the first order model (69) to the simulated data used in (a,b).

Fig. 7.— The amplitudes of subsequent harmonic terms for the relative delays D_1, D_2 (left and right panel respectively) corresponding to the planet I (a), II (b) and the parallactic motion (c).

Fig. 8.— Subsequent steps of the Frequency Decomposition for the simulated relative delay measurements between ν And and HD 10032 corresponding to the baseline vector orientation \mathbf{B}_1 . Left panel contains the residuals after removal of all components from the steps above. Right panel contains normalized periodograms of these residuals.

Fig. 9.— Continuation of Fig. 8

Table 1. Target star — v Andromedae (HD 9826, HIP 7513)

Parameter	v And	
Right ascension, α (J1991.25)	01 ^h 36 ^m 47 ^s .98	
Declination, δ (J1991.25)	41°24'23''00	
Proper motion in α , $\mu_\alpha \cos \delta$ (mas/yr)	-172.57	
Proper motion in δ , μ_δ (mas/yr)	-381.01	
Parallax, π (mas)	74.25	
Distance, d_{pc} (pc)	13.47	
Transverse velocity, V_T (km/s)	26.7	
Radial velocity, V_R (km/s)	-27.7	
Mass, M_\star (M_\odot)	1.3	
Orbital elements	Planet I	Planet II
Semi-major axis, a (AU)	0.83	2.5
Semi-major axis, $\hat{a} = \pi a m/M_\star$ (mas)	0.133	0.813
Orbital period, P (d)	241.2	1266.6
Eccentricity, e	0.18	0.41
Epoch of periastron, T_p (JD)	2450154.9	2451308.7
Longitude of periastron, ω	243°6	247°7
Longitude of ascending node, Ω	30°0	60°0
Inclination, i	45°0	45°0
Mass, m (M_{JUP})	2.95	5.98

Table 2. Reference star — HD 10032 (HIP 7672)

Parameter	HD 10032
Right ascension, α (J1991.25)	01 ^h 38 ^m 48 ^s .07
Declination, δ (J1991.25)	40°45'38''80
Proper motion in α , $\mu_\alpha \cos \delta$ (mas/yr)	-14.70
Proper motion in δ , μ_δ (mas/yr)	-2.66
Parallax, π (mas)	8.05
Distance, d_{pc} (pc)	124.22
Transverse velocity, V_T (km/s)	8.80
Radial velocity, V_R (km/s)	-34.00

Table 3. SIM orbital elements in SSB reference frame

Parameter	SIM
Semi-major axis, a (AU)	0.995
Orbital period, P (d)	362.5
Eccentricity, e	0.015
Epoch of periastron, T_p (JD) . .	2451519.44
Longitude of periastron, ω	74.°67
Longitude of ascending node, Ω	0.°005
Inclination, i	23.°45

Table 4. Dominant planetary terms from Frequency Decomposition

Parameter	Planet I	Planet II
f (1/d) . .	1/241.35	1/1265.87
\widehat{C}_1^1 (m) . . .	-0.743×10^{-11}	0.282×10^{-7}
\widehat{S}_1^1 (m) . . .	0.586×10^{-8}	0.790×10^{-9}
\widehat{C}_2^1 (m) . . .	-0.481×10^{-8}	0.756×10^{-8}
\widehat{S}_2^1 (m) . . .	0.146×10^{-8}	0.329×10^{-7}
\widehat{C}_1^2 (m) . . .	0.198×10^{-9}	-0.301×10^{-8}
\widehat{S}_1^2 (m) . . .	-0.683×10^{-9}	0.466×10^{-8}
\widehat{C}_2^2 (m) . . .	0.492×10^{-9}	-0.624×10^{-8}
\widehat{S}_2^2 (m) . . .	-0.148×10^{-9}	-0.202×10^{-8}

Table 5. Orbital elements derived from FD parameters

Parameter	Planet I	Planet II
Semi-major axis, \hat{a} (mas)	0.130	0.733
Orbital period, P (d)	241.35	1265.87
Eccentricity, e	0.22	0.39
Epoch of periastron, T_p (JD) ..	2450164.79	2451301.97
Longitude of periastron, ω	255°05	243°15
Longitude of ascending node, Ω	31°09	62°95
Inclination, i	44°50	43°13

Table 6. Orbital elements from standard model

Parameter	Planet I	Planet II
Semi-major axis, \hat{a} (AU)	0.132	0.813
Orbital period, P (d)	241.21	1265.65
Eccentricity, e	0.17	0.41
Epoch of periastron, T_p (JD) ..	2450152.63	2451306.95
Longitude of periastron, ω	240°34	247°88
Longitude of ascending node, Ω	29°65	59°96
Inclination, i	44°91	45°04

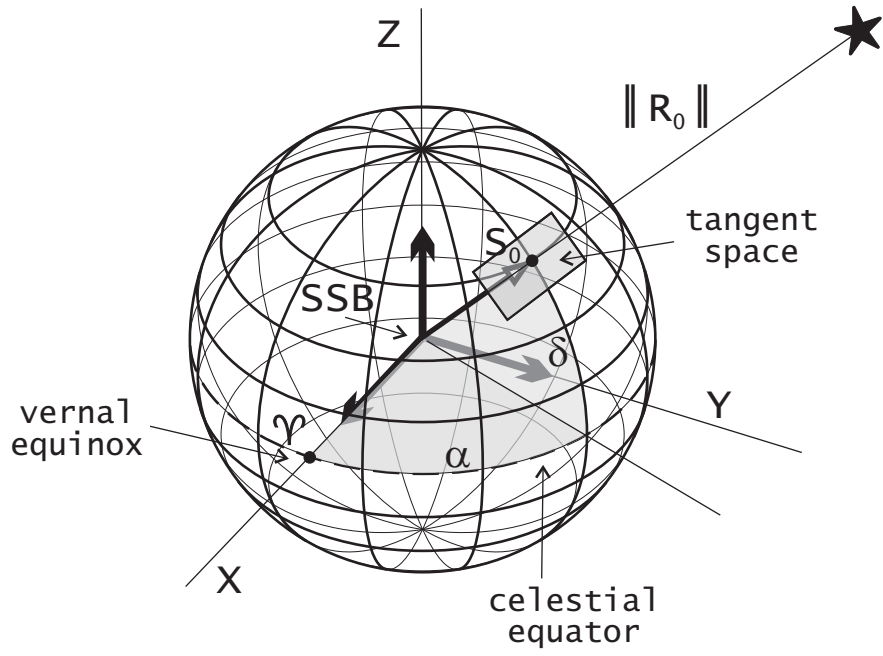


Fig. 1.—

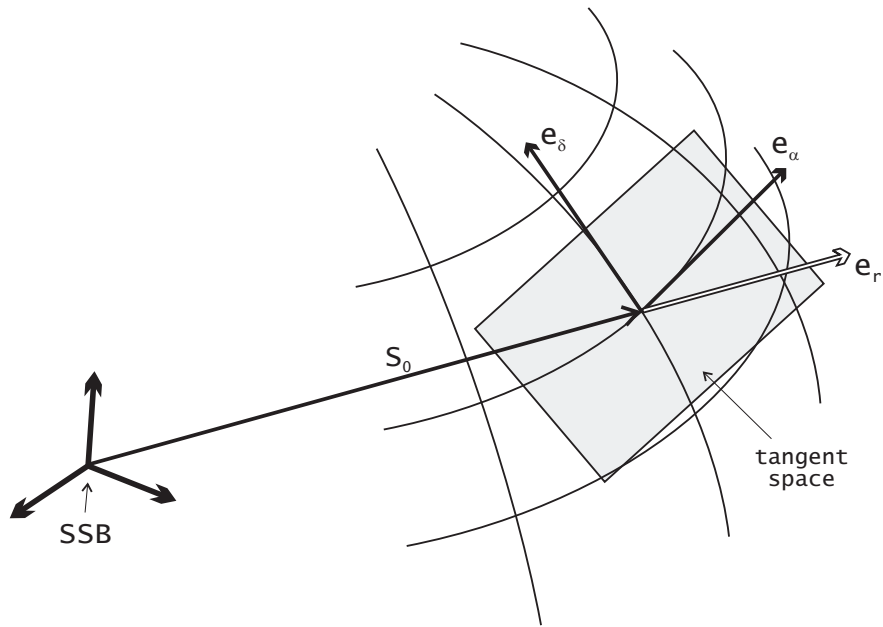


Fig. 2.—

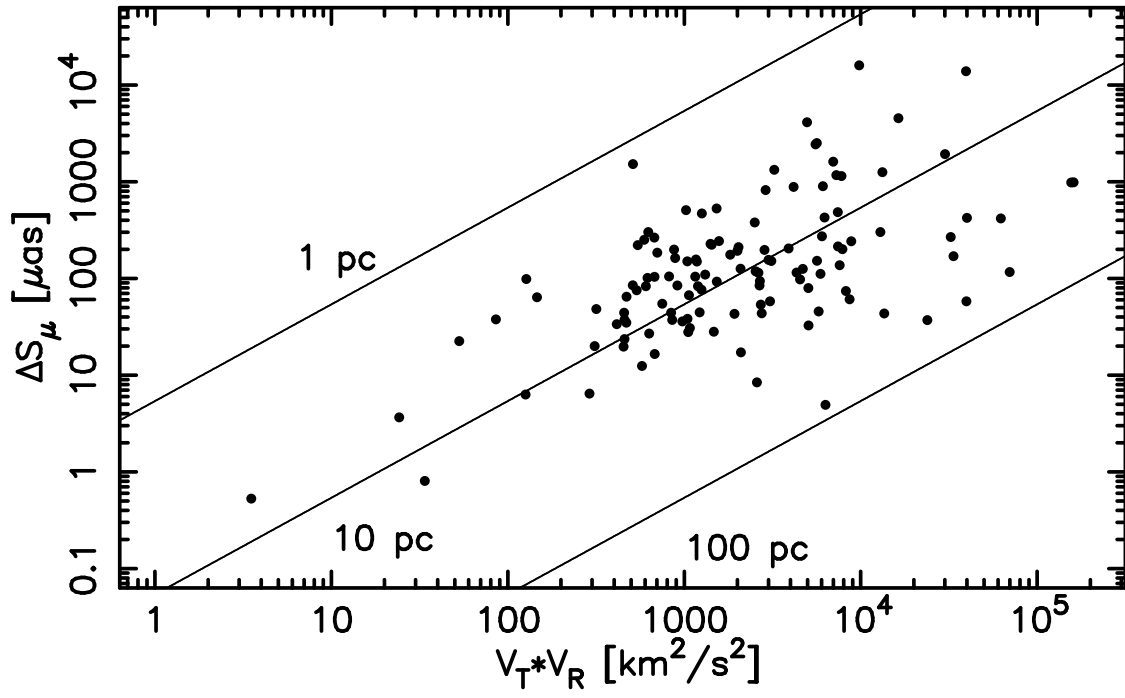


Fig. 3.—

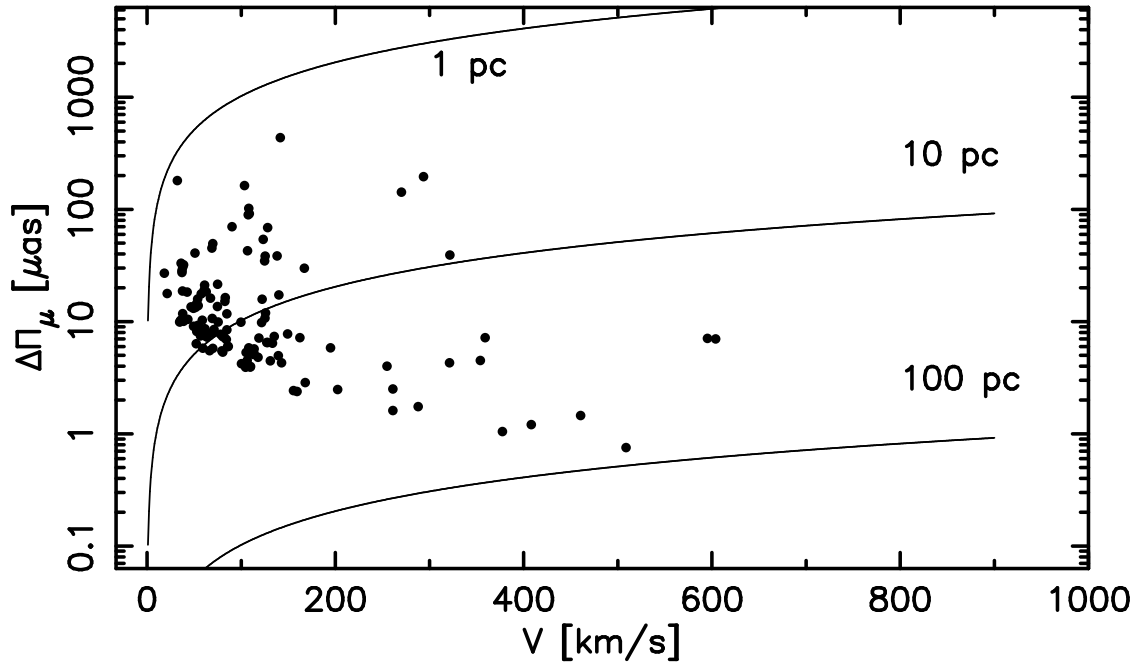


Fig. 4.—

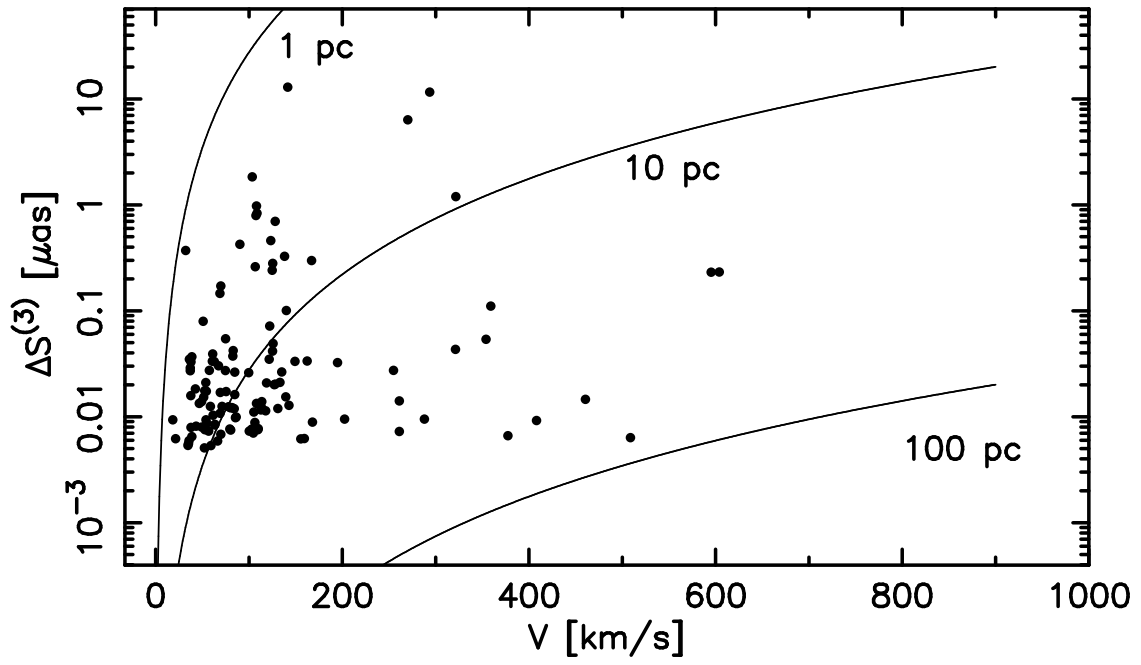


Fig. 5.—

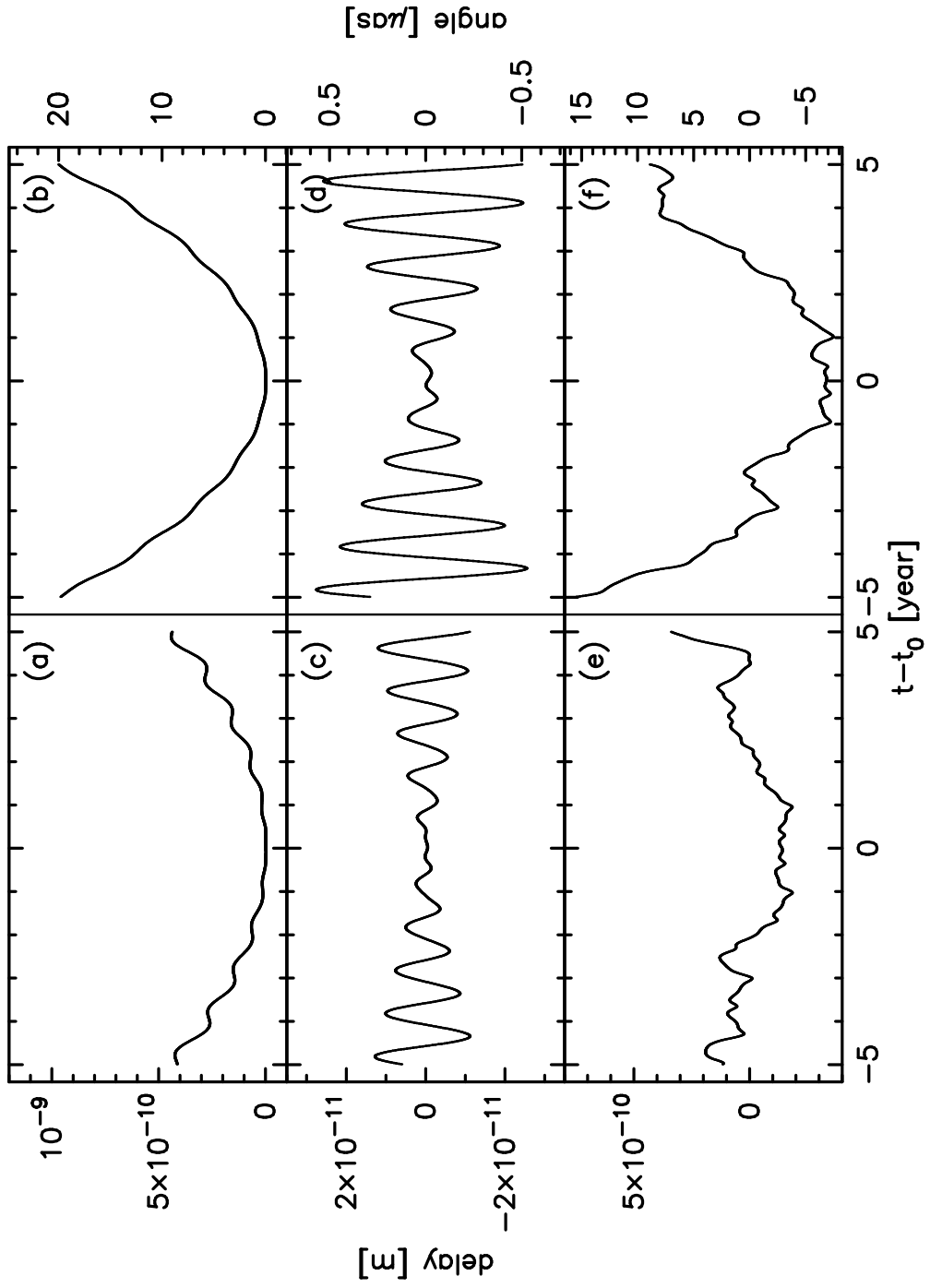


Fig. 6.—

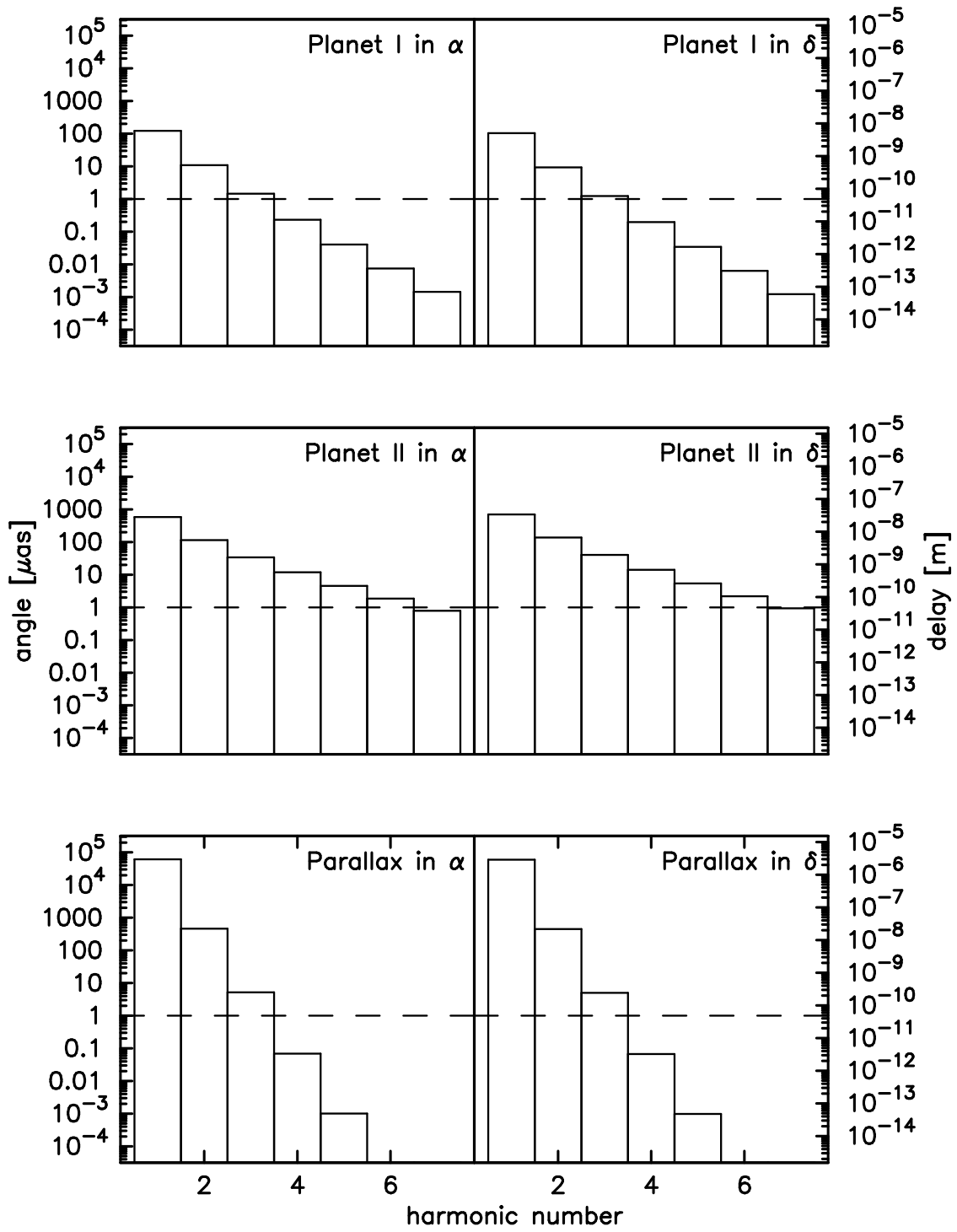


Fig. 7.—

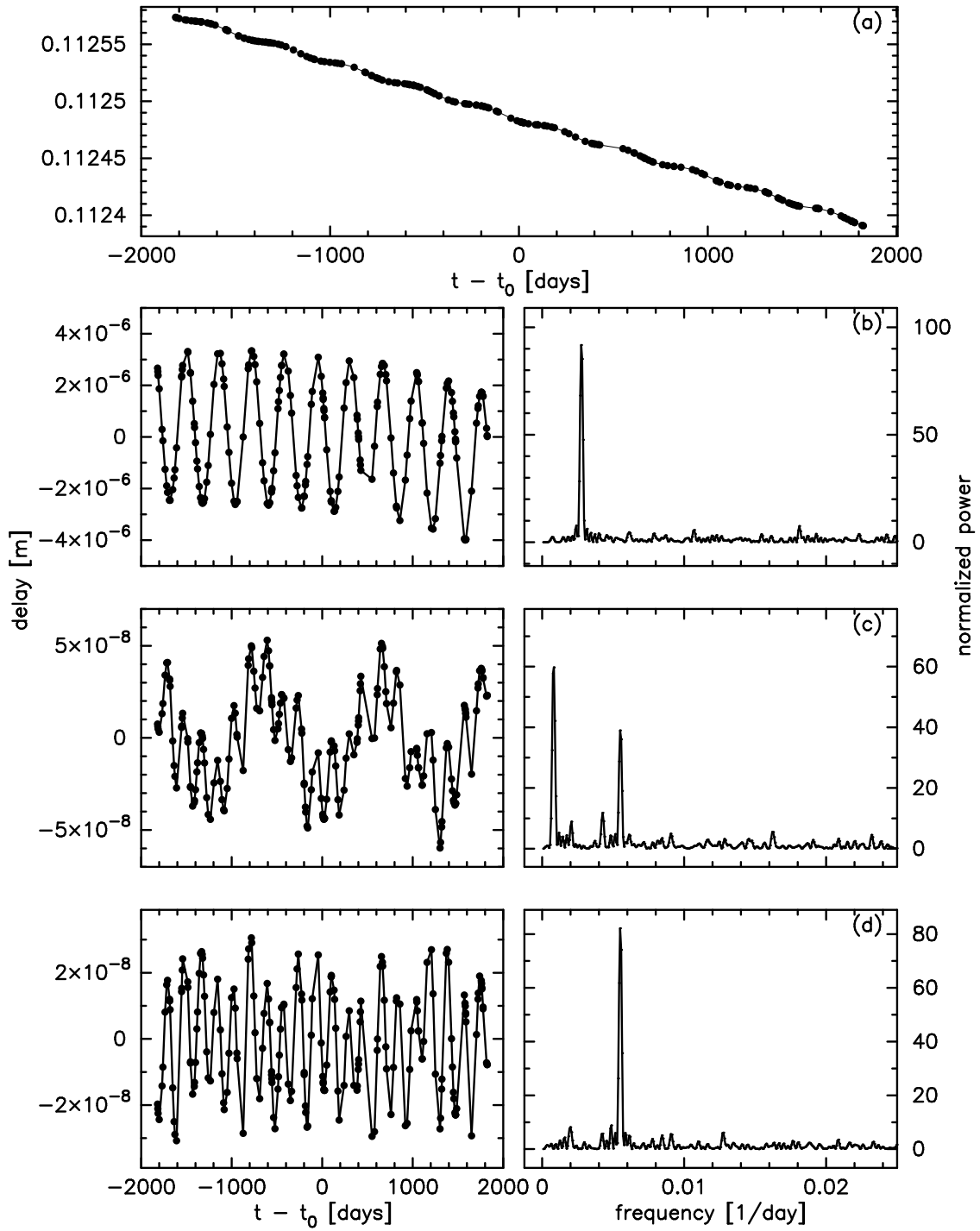


Fig. 8.—

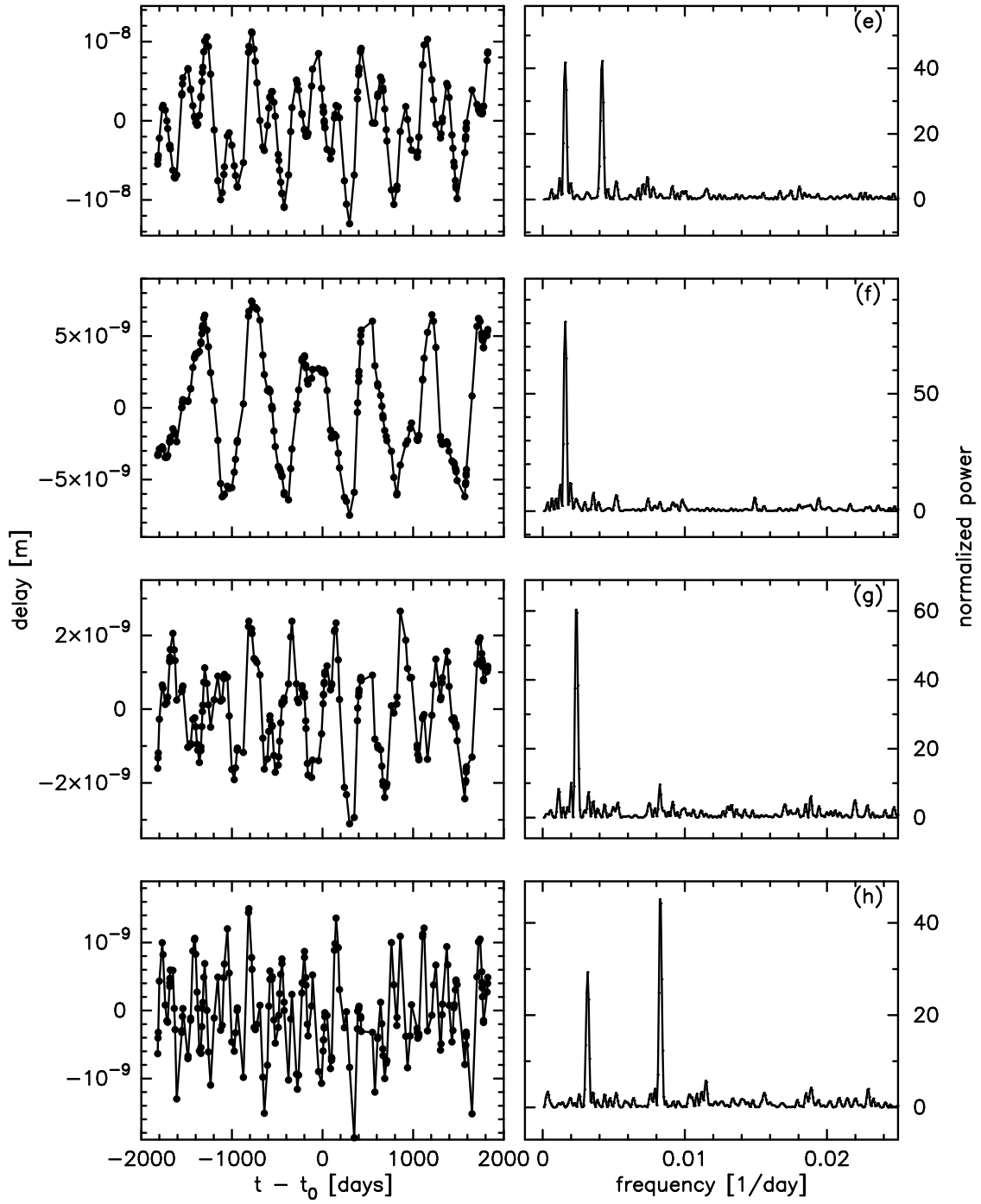


Fig. 9.—